Microbiota. 2024 September; 1(3): e154535 https://doi.org/10.5812/jmb-154535

Published Online: 2024 October 27 **Research Article**

Study the Antifungal Effects of Green Synthesized Silver Nanoparticles on the *Aspergillus niger*, *Microsporum canis*, and *Candida albicans*

Mohammad Mehdi Asgari Pirbalouti [1], Shahrzad Shahbazi [2], Somayeh Shahrokh Shahraki [1,*], Somayeh Reiisi [3], Azam Mokhtari [1]

[1] Department of Pathobiology, Faculty of Veterinary Medicine, Shahrekord University, Shahrekord, Iran
[2] Division of Genetics, Department of Cell and Molecular Biology and Microbiology, Faculty of Biological Science and Technology, University of Isfahan, Isfahan, Iran
[3] Department of Genetics, Faculty of Basic Sciences, Shahrekord University, Shahrekord, Iran

[*] ***Corresponding Author:*** Department of Pathobiology, Faculty of Veterinary Medicine, Shahrekord University, Shahrekord, Iran. Email: somaye.shahrokh@yahoo.com

Received: 14 September, 2024; **Revised:** 28 September, 2024; **Accepted:** 29 September, 2024

Abstract

The increasing prevalence of drug-resistant fungal pathogens and the limitations of current antifungal therapies underscore the need for novel alternative treatments. This study aimed to evaluate the antifungal effects of green-synthesized silver nanoparticles (Ag NPs) on three clinically significant fungi: *Aspergillus niger*, *Microsporum canis*, and *Candida albicans*. Silver nanoparticles were synthesized using plant-based extracts to ensure eco-friendly production methods. The synthesized Ag NPs were characterized using UV spectrophotometry, Fourier transform infrared spectroscopy (FTIR), X-ray diffraction (XRD), dynamic light scattering (DLS), zeta potential measurements, scanning electron microscopy (SEM), and transmission electron microscopy (TEM). Characterization assays revealed spherical particles with colloidal stability, an average size of approximately 80 nm, a Polydispersity Index of 0.4, and a surface charge of 62.3 mV. Minimum inhibitory concentration (MIC) values demonstrated effective suppression of fungal growth at low nanoparticle concentrations. In conclusion, our study highlights the potential of green-synthesized Ag NPs as a promising alternative to conventional antifungal agents, emphasizing their significant advantages in biocompatibility and eco-friendliness. These findings could pave the way for a new era in treating fungal infections, particularly those caused by drug-resistant strains.

Keywords: Silver Nanoparticle, Green Synthesis, Silymarin, *Aspergillus niger*, *Microsporum canis*, *Candida albicans*

1. Background

Fungal infections can cause various invasive and systemic disorders and have become a significant risk factor, especially for individuals with immune-associated disorders and pregnant women. Several antifungal drugs are widely used to treat these infections; however, their effectiveness is increasingly limited due to toxicity, drug resistance, and environmental concerns. Pathogenic fungi such as *Aspergillus niger*, *Microsporum canis*, and *Candida albicans* pose a serious threat to human health, particularly in immunocompromised individuals. These fungi are responsible for several major diseases and recent cases of resistance to the main antifungal drugs. While antifungal drug resistance may not seem as urgent as antibacterial drug resistance, the long-term issue lies in the limited availability of antifungal agents since fungi are eukaryotic organisms with structures and metabolic processes similar to those of their eukaryotic hosts. Consequently, there is an urgent need to identify novel antimicrobial agents (1, 2).

Nanomaterials, an advancement in nanotechnology, have been reported to exert antifungal activities and can be considered a tool for controlling phytopathogenic fungi (3). Among these, metal nanoparticles particularly silver, gold, copper, platinum, and palladium have been extensively studied for their antifungal properties. Silver nanoparticles (Ag NPs), in particular, can be used as biosensors, catalysts, drug delivery agents, antioxidants, and anticancer agents. They have gained significant attention due to their broad-spectrum antimicrobial properties. The small size, high surface-to-volume ratio, and ability to interact with microbial membranes make Ag NPs highly effective in combating resistant pathogens, including fungi. In addition to their

antimicrobial properties, Ag NPs have shown promise in a variety of applications, ranging from medical diagnostics to environmental remediation, highlighting their versatility and potential as a powerful tool in science and technology (4).

Silver nanoparticles can be synthesized through various methods, including physical, chemical, electrochemical, microwave-assisted synthesis, and photochemical reductions (5-7). However, these methods face limitations, including the use of ecotoxic chemical agents like reducing and stabilizing agents, the need for sophisticated facilities, and harsh, expensive conditions such as high temperatures and vacuum technology (5, 8). To overcome these limitations, biosynthetic methods have been developed using plant extracts, enzymes, flavonoids, and microorganisms such as fungi and actinomycetes (9, 10) These techniques, often referred to as "green synthesis of nanoparticles," are characterized by their eco-friendly nature, non-toxic properties, enhanced biocompatibility, and cost-effectiveness, reducing the need for advanced instruments (11).

In this study, we assessed the antifungal effects of green-synthesized Ag NPs using silymarin (SLM) on three clinically relevant fungal species: *Aspergillus niger*, a common cause of aspergillosis; *M. canis*, responsible for dermatophyte infections; and *C. albicans*, a significant pathogen in systemic candidiasis.

2. Objectives

By investigating the efficacy of these green-synthesized Ag NPs, we aimed to evaluate their potential as alternative antifungal treatments with lower environmental risks and toxicity.

3. Methods

3.1. Synthesis of Silver Nanoparticles

Silymarin (Sigma-Aldrich, Germany) was used as a reducing agent for the green synthesis of Ag NPs. The synthesis protocol involved preparing a 20 mM silver nitrate ($AgNO_3$) (Sigma-Aldrich, Germany) solution in 2 mL of distilled water and a 10 mM SLM solution in 2 mL of ethanol. To initiate the reaction, 2 mL of the $AgNO_3$ solution was added to 46 mL of deionized water under continuous stirring. The SLM solution was then introduced dropwise into the reaction mixture. The pH of the mixture was adjusted to 11 using sodium hydroxide (NaOH), followed by stirring at 1000 rpm for 1 hour. The resulting dark black solution, indicative of Ag NP formation, was centrifuged at 4°C and 12,000 rpm for 20 minutes to collect the nanoparticle precipitate. The concentration of the synthesized Ag NPs was determined using inductively coupled plasma spectroscopy, initially quantified in parts per billion (ppb) and converted to micrograms. Various concentrations of Ag NPs were prepared to establish a calibration curve, with the absorbance measured at 400 nm using UV-Vis spectrophotometry (12).

3.2. Characterization of Synthesized Nanoparticles

The particle size, Polydispersity Index (PDI), and zeta potential of the Ag NPs were measured using dynamic light scattering (DLS) with an SZ-100 nanoparticle analyzer (Horiba, Japan). The crystalline structure of the synthesized Ag NPs was characterized by X-ray diffraction (XRD) analysis, performed on a D8 ADVANCE X-ray diffractometer (Bruker, Germany) at a scanning rate of 15°/min across a diffraction angle range of 10 - 90°C. Functional groups and chemical properties were further assessed using Fourier transform infrared (FTIR) spectroscopy, conducted with an FT/IR-6300 spectrometer (JASCO, Japan) over a scanning range of 350 - 4000 cm^{-1}. The morphology of the Ag NPs was examined via scanning electron microscopy (SEM; JSM6701F, JEOL, Japan) and transmission electron microscopy (TEM; CM120, Philips, Netherlands) (13).

3.3. Determination of Minimum Inhibitory Concentration

To assess the antifungal efficacy of varying concentrations of Ag NPs against *A. niger*, *M. canis*, and *C. albicans*, the minimum inhibitory concentration (MIC) was determined. In this method, *C. albicans* was cultured in Mueller-Hinton broth (MHB) (Sigma-Aldrich, Germany) medium and treated with increasing concentrations (6-fold dilutions) of the respective nanoparticle. The positive control well contained *C. albicans* and the culture medium, while the negative control well contained only the initial stock of the compound and the medium. The microplates were shaken for 30 seconds to ensure a homogeneous mixture and then incubated at 37°C for 18 hours. The MIC was determined as the lowest concentration of the compound that showed no turbidity, indicating inhibition of microbial growth. Turbidity was compared with the positive control well, while transparency and clarity were compared to the negative control well.

For *A. niger* and *M. canis*, the fungi were cultured in Mueller-Hinton agar (MHA) (Sigma-Aldrich, Germany) and treated with serial dilutions of Ag NPs. The positive control plate contained the target microorganism and culture medium, while the negative control plate contained the Ag NPs stock solution and medium. The

plates were incubated at 37°C for 24 hours. The MIC was defined as the lowest concentration of Ag NPs that exhibited no fungal growth, indicating successful inhibition of microbial proliferation.

4. Results

4.1. Silver Nanoparticles Biosynthesis and Characterization

As previously described, Ag NPs were synthesized using a green method with SLM. The formation of Ag NPs was visually confirmed through a color change during the reaction. As shown in Figure 1, the solution changed from light yellow (Figure 1A) to blackish brown (Figure 1B), indicating the reduction of silver ions (Ag^{+}) to elemental silver (Ag^{0}).

The successful synthesis of Ag NPs was further validated by UV-visible spectrophotometry. Figure 1C shows a broad absorption peak at approximately 410 nm, which confirms the formation of Ag NPs.

The colloidal stability of the Ag NPs was evaluated using DLS and zeta potential measurements. As shown in Figure 2A, the hydrodynamic diameter of the green-synthesized Ag NPs was approximately 80 nm, with a PDI of 0.4, indicating a moderate distribution of particle sizes.

Additionally, the zeta potential of the synthesized Ag NPs, as displayed in Figure 2B, was approximately -44 mV. This high zeta potential value indicates strong electrostatic repulsion between the particles, contributing to the stability of the colloidal suspension and preventing nanoparticle agglomeration.

The XRD patterns, illustrated in Figure 2C, show two prominent and well-defined reflections at 2θ values of approximately 38.78° and 65.14°, corresponding to lattice spacings (d_hkl) of 2.35 Å and 1.45 Å, respectively. These diffraction peaks confirm the face-centered cubic (fcc) crystalline structure of silver. Specifically, the peaks at 2θ 38.78° and 65.14° correspond to the (111) and (220) crystallographic planes of the fcc lattice.

The FTIR spectrum highlights the key functional groups involved in the green synthesis and stabilization of Ag NPs using SLM as both a reducing and capping agent (Figure 2D). As shown in Figure 3, a broad absorption band around 3400 cm^{-1} corresponds to O–H and N–H stretching vibrations, indicative of hydroxyl and amine groups. These groups, derived from bioactive compounds such as flavonoids and proteins present in SLM, play a crucial role in reducing silver ions (Ag^{+}) to elemental silver (Ag^{0}). Hydroxyl groups, in particular, act as electron donors, facilitating the reduction process. The peak observed at 2900 cm^{-1}, associated with C–H stretching, suggests the presence of alkyl chains, likely from organic compounds in the SLM extract, which may contribute to the hydrophobic stabilization of Ag NPs.

Additionally, the sharp peak at 1650 cm^{-1} corresponds to C=O stretching, indicating the presence of carbonyl groups, potentially from amides or other carbonyl-containing molecules. These carbonyl groups interact with the nanoparticle surface, further enhancing stabilization by preventing agglomeration. Peaks around 1400 cm^{-1} are attributed to C–H bending and aromatic C=C stretching, suggesting the presence of aromatic compounds. These possible flavonoids may contribute to nanoparticle stabilization through π-π interactions. Finally, the sharp absorption band in the range of 1000 - 1200 cm^{-1} indicates C–O stretching, typically associated with alcohols or ethers, confirming the role of these groups in the capping and stabilization of Ag NPs.

Figure 3 presents the morphology of the synthesized Ag NPs, as visualized through scanning electron microscopy (SEM) (Figure 3A) and transmission electron microscopy (TEM) (Figure 3B) imaging. The SEM images revealed that the Ag NPs were predominantly spherical with a relatively uniform size distribution. The particles displayed smooth surfaces with occasional aggregates, indicating successful synthesis with minimal agglomeration. The average particle size observed in the SEM images aligned with the hydrodynamic diameter obtained from DLS measurements. Transmission electron microscopy analysis provided a more detailed view of the internal structure of the Ag NPs, confirming their spherical shape with well-defined boundaries, further supporting the uniformity in particle size and shape observed in the SEM analysis.

4.2. Determination of Minimum Inhibitory Concentration

This study investigated the antifungal activity of green-synthesized Ag NPs against *C. albicans* using the broth microdilution technique, and against *A. niger* and *M. canis* using plate assays. The microbial stock, obtained from overnight fungal cultures, was inoculated onto plates and incubated at 32°C for 24 hours. A gradient of Ag NPs concentrations (10, 20, 40, 80, 160, 320, and 640 μg/mL) was used to determine the MIC, with serial dilutions performed to identify the lowest concentration that inhibited fungal growth.

As shown in Figure 4A, a dark color is visible in the lower wells, likely corresponding to higher concentrations of Ag NPs, possibly indicating complete inhibition of fungal growth. As the concentration decreases across the wells, the color becomes lighter

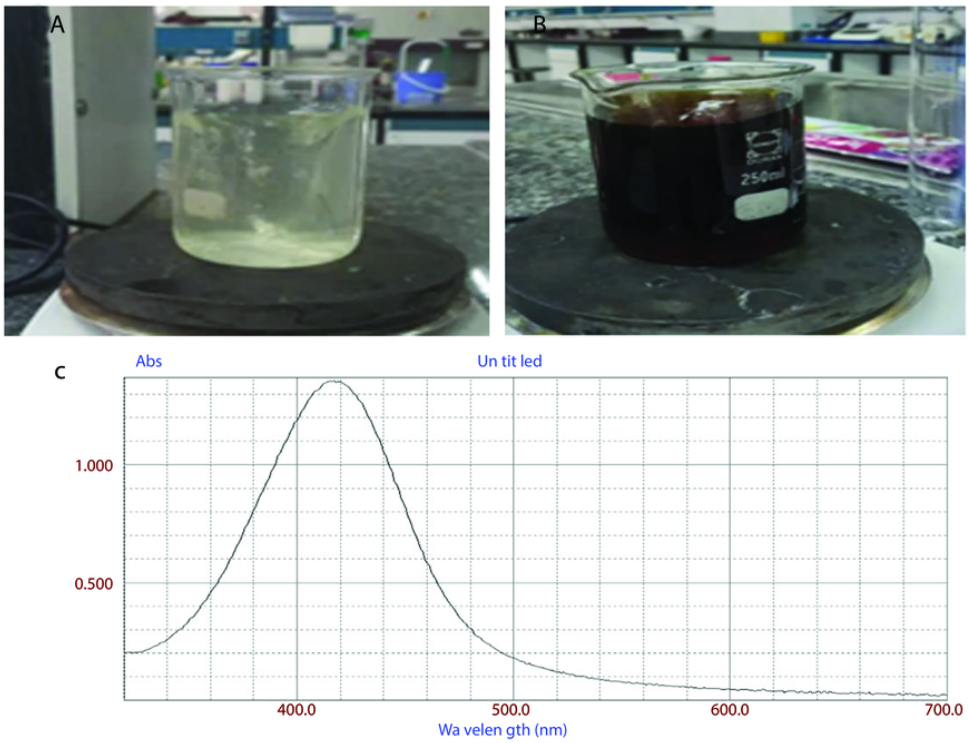

Figure 1. A and B, green synthesis of silver nanoparticles (Ag NPs) using silymarin (SLM); C, UV-Vis absorption spectra of green synthesized Ag NPs using SLM

and more transparent, suggesting a reduction in the inhibitory effect and possible fungal growth. This assay demonstrates a dose-dependent antifungal effect, where increasing concentrations of Ag NPs result in more significant inhibition of *C. albicans*. Moreover, based on the broth microdilution, the MIC for *C. albicans* revealed that concentrations as low as 80 µg/mL effectively inhibited growth.

For *A. niger* and *M. canis*, plate assays revealed significant inhibition of fungal growth at Ag NPs concentrations starting from 320 µg/mL for *A. niger* and 80 µg/mL for *M. canis* (Figure 4A and B, respectively).

5. Discussion

In this study, Ag NPs were synthesized using an eco-friendly method with SLM as a reducing and stabilizing agent, indicated by a color change from light yellow to blackish brown, signifying the reduction of silver ions (Ag^{+}) to elemental silver (Ag^{0}). This dual function of SLM is attributed to its bioactive compounds such as alkaloids, flavonoids, saponins, and steroids (14). The successful synthesis of the Ag NPs was validated using various analytical techniques. The FTIR results confirmed the involvement of hydroxyl, amine, carbonyl, and ether groups in both the reduction and stabilization of Ag NPs. These bioactive molecules not only facilitated the reduction process but also provided a stable environment to prevent nanoparticle aggregation, consistent with previous studies on green nanoparticle synthesis (15-18).

X-ray diffraction analysis revealed sharp and narrow reflections, confirming the high crystallinity of the Ag NPs synthesized in this study. According to previous research, a low PDI suggests a narrow size distribution, indicating a uniform size for the synthesized Ag NPs (19). In this study, DLS and zeta potential measurements showed that the hydrodynamic diameter of the green-synthesized Ag NPs was approximately 80 nm, with a PDI of 0.4. As demonstrated in prior studies, a low PDI suggests a relatively narrow size distribution and uniform size of the Ag NPs (19). Additionally, the surface charge of the green-synthesized Ag NPs was approximately 62.3 mV. This positive potential value can be attributed to the interaction between SLM and the

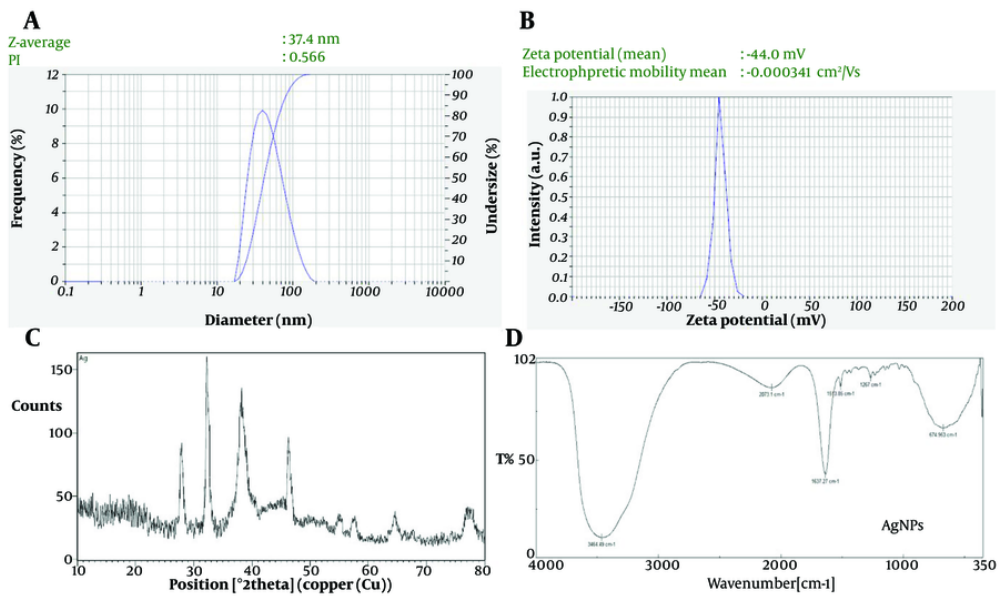

Figure 2. A, dynamic light scattering (DLS) result for silver nanoparticles (Ag NPs); B, ZETA graph for net charge of Ag NPs; C, X-ray diffraction (XRD), pattern of green synthesized Ag NPs using SLM; D, FTIR pattern of green synthesized Ag NPs using SLM

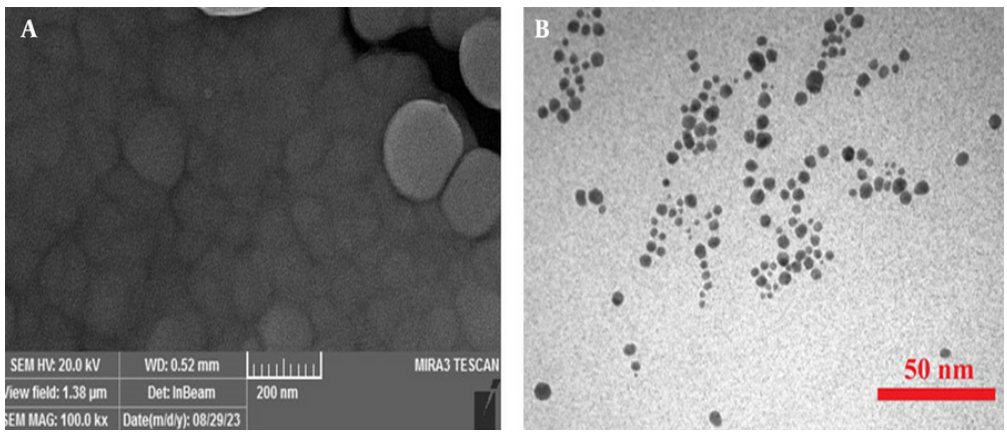

Figure 3. Morphological analysis using Fe- scanning electron microscopy (SEM) (A) and transmission electron microscopy (TEM) (B)

surface of the Ag NPs, potentially altering the surface charge distribution. The functional groups in SLM may contribute to a net positive charge or affect surface chemistry. This observation aligns with previous studies on the impact of natural compounds on nanoparticle charge and stability (20, 21). Moreover, the morphological analysis confirmed a predominantly spherical and relatively uniform size distribution for the green-synthesized Ag NPs, consistent with the findings of Mekky et al. and Ogbogo et al., who reported similar results using *Spinacia oleracea* and *Jatropha curcas* leaves as source plants, respectively (20, 22).

Silver nanoparticles are known for their broad-spectrum antifungal properties, attributed to their

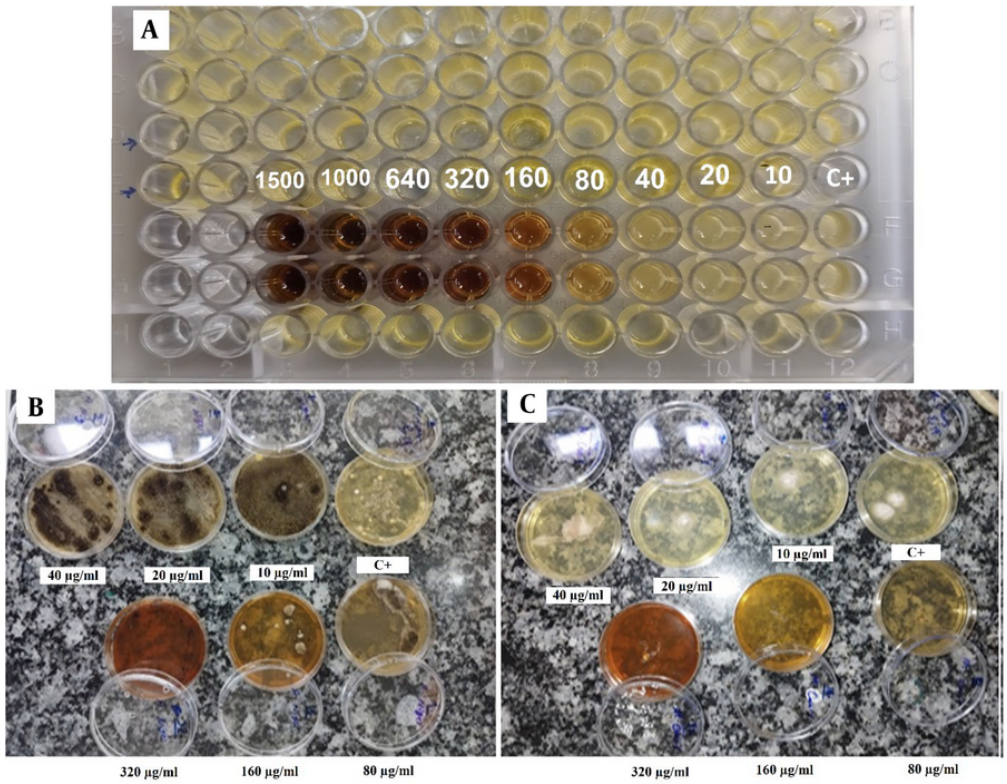

Figure 4. Plate assays for A, *Candida albicans*; B, *Aspergillus niger*; and C, *Microsporum canis* in treatment with silver nanoparticles (Ag NPs)

small size, high surface area-to-volume ratio, and ability to penetrate fungal cell walls, causing cellular damage and death (23). This study employed the broth microdilution technique to assess the antifungal efficacy of green-synthesized Ag NPs against *C. albicans*. The results demonstrated a dose-dependent antifungal effect, with increasing concentrations of Ag NPs resulting in enhanced inhibition of *A. niger*, *M. canis*, and *C. albicans*. These findings align with previous studies highlighting the potent antifungal properties of Ag NPs, which are known to disrupt fungal cell walls and membranes, leading to cytoplasmic leakage and cell death (24).

Moreover, another study has shown that Ag NPs interact with fungal cells to generate reactive oxygen species (ROS), which further contributes to cellular damage and death (25). In this study, the MIC for *C. albicans* was found to be 80 µg/mL, consistent with earlier studies that reported MIC values for biosynthesized Ag NPs against *Candida* species ranging from 62.5 to 125 µg/mL (26). For *A. niger* and *M. canis*, plate assays revealed significant growth inhibition at concentrations starting from 320 µg/mL and 80 µg/mL, respectively (Figure 4A and B). Previous research has typically reported MIC values for *Aspergillus* species within the range of 62.5 to 125 µg/mL.

Overall, the MIC values observed in this study are comparable to those in other studies where Ag NPs, synthesized using various biological sources and methods, exhibited strong antifungal activity at concentrations as low as 15.62 to 125 µg/mL, depending on the fungal species and the plant extract used for the green synthesis of the Ag NPs (25).

5.1. Conclusions

In conclusion, this study demonstrated the potent antifungal activity of green-synthesized Ag NPs using SLM against *A. niger*, *M. canis*, and *C. albicans*. The results showed that these green-synthesized Ag NPs effectively inhibited the growth of all three fungal species, with MICs consistent with recent studies. These findings

suggest that green-synthesized Ag NPs hold significant potential as alternative antifungal agents, especially in addressing resistant fungal strains, and their application could be further explored in clinical settings.

Footnotes

Authors' Contribution: Study concept and design: M. P. and S. S.; analysis and interpretation of data: S. R. and A. M.; drafting of the manuscript: Sh. Sh.; critical revision of the manuscript for important intellectual content: S. S., S. R., and A. M.; statistical analysis: S. R.

Conflict of Interests Statement: The authors declared no conflict of interests.

Data Availability: The data set presented in the study is available on request from the corresponding author during submission or after publication. The data are not publicly available due to our policy.

Funding/Support: This study was supported in part by grant 1GRN3650457 from Shahrekord University by a teaching and research scholarship from the faculty of veterinary medicine.

References

1. Vitiello A, Ferrara F, Boccellino M, Ponzo A, Cimmino C, Comberiati E, et al. Antifungal Drug Resistance: An Emergent Health Threat. *Biomed*. 2023;**11**(4). [PubMed ID: 37189681]. [PubMed Central ID: PMC10135621]. https://doi.org/10.3390/biomedicines11041063.
2. Nasrollahi A, Pourshamsian K, Mansourkiaee P. Antifungal activity of silver nanoparticles on some of fungi. *Int J Nano Dim*. 2010;**1**. https://doi.org/10.7508/ijnd.2010.03.007.
3. Shinde BH, Inamdar S, Nalawade SA, Chaudhari SB. A systematic review on antifungal and insecticidal applications of biosynthesized metal nanoparticles. *Mater Today Proceed*. 2023;**73**:412-7. https://doi.org/10.1016/j.matpr.2022.09.548.
4. Gong X, Jadhav ND, Lonikar VV, Kulkarni AN, Zhang H, Sankapal BR, et al. An overview of green synthesized silver nanoparticles towards bioactive antibacterial, antimicrobial and antifungal applications. *Adv Colloid Interface Sci*. 2024;**323**:103053. [PubMed ID: 38056226]. https://doi.org/10.1016/j.cis.2023.103053.
5. Ashkarran AA. A novel method for synthesis of colloidal silver nanoparticles by arc discharge in liquid. *Curr App Physic*. 2010;**10**(6):1442-7. https://doi.org/10.1016/j.cap.2010.05.010.
6. Lim PY, Liu RS, She PL, Hung CF, Shih HC. Synthesis of Ag nanospheres particles in ethylene glycol by electrochemical-assisted polyol process. *Chem Physic Letter*. 2006;**420**(4-6):304-8. https://doi.org/10.1016/j.cplett.2005.12.075.
7. Darmanin T, Nativo P, Gilliland D, Ceccone G, Pascual C, De Berardis B, et al. Microwave-assisted synthesis of silver nanoprisms/nanoplates using a "modified polyol process". *Colloids Surface Physicochem Eng Aspect*. 2012;**395**:145-51. https://doi.org/10.1016/j.colsurfa.2011.12.020.
8. Kumar D, Kumar P, Singh H, Agrawal V. Biocontrol of mosquito vectors through herbal-derived silver nanoparticles: prospects and challenges. *Environ Sci Pollut Res Int*. 2020;**27**(21):25987-6024. [PubMed ID: 32385820]. https://doi.org/10.1007/s11356-020-08444-6.
9. Shaik M, Khan M, Kuniyil M, Al-Warthan A, Alkhathlan H, Siddiqui M, et al. Plant-Extract-Assisted Green Synthesis of Silver Nanoparticles Using Origanum vulgare L. Extract and Their Microbicidal Activities. *Sustainability*. 2018;**10**(4). https://doi.org/10.3390/su10040913.
10. Vishwanath R, Negi B. Conventional and green methods of synthesis of silver nanoparticles and their antimicrobial properties. *Curr Res Green Sustainable Chem*. 2021;**4**. https://doi.org/10.1016/j.crgsc.2021.100205.
11. Arroyo GV, Madrid AT, Gavilanes AF, Naranjo B, Debut A, Arias MT, et al. Green synthesis of silver nanoparticles for application in cosmetics. *J Environ Sci Health A Tox Hazard Subst Environ Eng*. 2020;**55**(11):1304-20. [PubMed ID: 32715864]. https://doi.org/10.1080/10934529.2020.1790953.
12. Chelegahi AM, Reiisi S, Heidari R, Karimi B. Novel Silymarin-Loaded Biosynthesized AgNPs for Improving Anticancer Activities in Breast Cancer. *Bio Nano Sci*. 2023;**13**(4):1817-32. https://doi.org/10.1007/s12668-023-01183-1.
13. Arghand N, Reiisi S, Karimi B, Khorasgani EM, Heidari R. Biosynthesis of Nanocomposite Alginate-Chitosan Loaded with Silver Nanoparticles Coated with Eugenol/Quercetin to Enhance Wound Healing. *Bio Nano Sci*. 2024;**2024**. https://doi.org/10.1007/s12668-024-01479-w.
14. Elhassaneen Y, Nasef A, Arafa R, Bayomi A. Bioactive compounds and antioxidant activities of milk thistle (*Silybum marianum*) extract and their potential roles in the prevention of diet-induced obesity complications. *America J Food Sci Technol*. 2023;**11**(3):70-85. https://doi.org/10.12691/ajfst-11-3-1.
15. Iravani S. Green synthesis of metal nanoparticles using plants. *Green Chem*. 2011;**13**(10). https://doi.org/10.1039/c1gc15386b.
16. Sharma VK, Yngard RA, Lin Y. Silver nanoparticles: green synthesis and their antimicrobial activities. *Adv Colloid Interface Sci*. 2009;**145**(1-2):83-96. [PubMed ID: 18945421]. https://doi.org/10.1016/j.cis.2008.09.002.
17. Singh P, Kim YJ, Zhang D, Yang DC. Biological Synthesis of Nanoparticles from Plants and Microorganisms. *Trends Biotechnol*. 2016;**34**(7):588-99. [PubMed ID: 26944794]. https://doi.org/10.1016/j.tibtech.2016.02.006.
18. Ahmed S, Ahmad M, Swami BL, Ikram S; Saifullah. Green synthesis of silver nanoparticles using Azadirachta indica aqueous leaf extract. *J Radiat Res Appl Sci*. 2016;**9**(1):1-7. https://doi.org/10.1016/j.jrras.2015.06.006.
19. Manosalva N, Tortella G, Cristina Diez M, Schalchli H, Seabra AB, Duran N, et al. Green synthesis of silver nanoparticles: effect of synthesis reaction parameters on antimicrobial activity. *World J Microbiol Biotechnol*. 2019;**35**(6):88. [PubMed ID: 31134435]. https://doi.org/10.1007/s11274-019-2664-3.
20. Mekky A, Farrag A, Sofy A, Hamed A. Antibacterial and Antifungal Activity of Green-synthesized Silver Nanoparticles Using Spinacia oleracea leaves Extract. *Egypt J Chem*. 2021;**0**(0):0. https://doi.org/10.21608/ejchem.2021.74432.3673.
21. Patil SV, Borase HP, Patil CD, Salunke BK. Biosynthesis of silver nanoparticles using latex from few Euphorbian plants and their antimicrobial potential. *Appl Biochem Biotechnol*. 2012;**167**(4):776-90. [PubMed ID: 22592777]. https://doi.org/10.1007/s12010-012-9710-z.
22. Ogbogo OI, Ikyenge AB, Ishwah B, Weor TT, Adoga OS. Synthesis, Characterization and Antibacterial Activity Studies of Eco-Friendly Silver Nanoparticles from the Leaf Extract of Jatropha Curcas. *Schol Int J Chem Mater Sci*. 2022;**5**(8):128-34. https://doi.org/10.36348/sijcms.2022.v05i08.001.
23. Rai M, Kon K, Ingle A, Duran N, Galdiero S, Galdiero M. Broad-spectrum bioactivities of silver nanoparticles: the emerging trends

and future prospects. *Appl Microbiol Biotechnol*. 2014;**98**(5):1951-61. [PubMed ID: 24407450]. [PubMed Central ID: PMC7080016]. https://doi.org/10.1007/s00253-013-5473-x.

24. Hassan SA, Hanif E, Khan UH, Tanoli AK. Antifungal activity of silver nanoparticles from Aspergillus niger. *Pak J Pharm Sci*. 2019;**32**(3 (Supplementary)):1163-6. [PubMed ID: 31303585].
25. Hashem AH, Saied E, Amin BH, Alotibi FO, Al-Askar AA, Arishi AA, et al. Antifungal Activity of Biosynthesized Silver Nanoparticles (AgNPs) against Aspergilli Causing Aspergillosis: Ultrastructure Study. *J Funct Biomater*. 2022;**13**(4). [PubMed ID: 36412883]. [PubMed Central ID: PMC9680418]. https://doi.org/10.3390/jfb13040242.
26. Klein W, Ismail E, Maboza E, Hussein AA, Adam RZ. Green-Synthesized Silver Nanoparticles: Antifungal and Cytotoxic Potential for Further Dental Applications. *J Funct Biomater*. 2023;**14**(7). [PubMed ID: 37504874]. [PubMed Central ID: PMC10381808]. https://doi.org/10.3390/jfb14070379.